processes

Article

Genesis Types and Migration of Middle and Lower Assemblages of Natural Gas in the Eastern Belt around the Penyijingxi Sag of the Junggar Basin, NW China

Keshun Liu [1], Jiangxiu Qu [1,*], Ming Zha [1], Hailei Liu [2], Xiujian Ding [1], Minghui Zhou [3] and Tianze Gao [1]

[1] School of Geosciences, China University of Petroleum (East China), Qingdao 266580, China
[2] Research Institute of Exploration and Development, PetroChina Xinjiang Oilfield Company, Karamay 834000, China
[3] Baikouquan Oil Production Plant, PetroChina Xinjiang Oilfield Company, Karamay 834000, China
* Correspondence: 20030040@upc.edu.cn

Abstract: This study analyzes the geochemical characteristics of natural gas composition, carbon isotope, and light hydrocarbon in the eastern belt around the Penyijingxi sag of the Junggar Basin. The result shows the that natural gas content is dominated by alkane gas, with low contents of heavy hydrocarbon and non-hydrocarbon components. The overall carbon isotopic composition of the alkanes shows a trend as δ^{13}methane (C_1) < δ^{13}ethane (C_2) < δ^{13}propane (C_3) < δ^{13}butane (C_4), and all $\delta^{13}C_1$ values are <−30‰, which are typical of gases of organic origin. The natural gas is mainly coal-derived gas from the Lower Urho formation, mixed with a small amount of oil-associated gas from the Fengcheng formation. The vertical migration of natural gas resulted in the mixing of oil-associated gas and coal-derived gas and the mixing of alkane gas at different stages of the same origin, which should be the origin of carbon isotope inversion. The diffusion migration of carboniferous oil and gas reservoirs has led to differences in gas geochemical characteristics among gas wells. These migration characteristics of natural gas may indicate that the shallow layers are a favorable stratum for the next step of oil and gas exploration in the eastern belt around the Penyijingxi sag.

Keywords: Junggar Basin; natural gas genesis; migration characteristics; carbon isotopes; light hydrocarbons

check for updates

Citation: Liu, K.; Qu, J.; Zha, M.; Liu, H.; Ding, X.; Zhou, M.; Gao, T. Genesis Types and Migration of Middle and Lower Assemblages of Natural Gas in the Eastern Belt around the Penyijingxi Sag of the Junggar Basin, NW China. *Processes* **2023**, *11*, 689. https://doi.org/10.3390/pr11030689

Academic Editors: Ping Gao, Yidong Cai, Yingfang Zhou and Quan Gan

Received: 3 February 2023
Revised: 20 February 2023
Accepted: 22 February 2023
Published: 24 February 2023

1. Introduction

There are two types of natural gas in sedimentary basins, inorganic and organic [1], and organic gas is further divided into oil-associated and coal-derived gas [2–4]. Inorganic gas is potentially associated with magmatic and deep-sea hydrothermal activity [5,6], with methane isotopes ($\delta^{13}C_1$) within the range of −50‰ (generally −30‰) to 10‰ [7,8], while organic gas is derived from the pyrolysis of kerogen in sedimentary rocks and the secondary cracking gas of crude oil, with methane isotopes in the range of −75‰ to −30‰ [7]. The inorganic alkane gas polymerized step-by-step to form long-chain alkanes through C-C bonding and the lower bond energy of ^{12}C-^{12}C caused ^{12}C to join the polymerization reaction first, showing a negative carbon isotope series of δ^{13}methane (C_1) > δ^{13}ethane (C_2) > δ^{13}propane (C_3) > δ^{13}butane (C_4) [9]. When alkane gas was generated from the degradation of kerogen, ^{12}C-^{12}C with lower bond energy broke preferentially than ^{13}C-^{13}C, leading to the gradual enrichment of $\delta^{13}C$ in organic alkane gas with the increase of the carbon atom number, thus forming a positive carbon isotope series of $\delta^{13}C_1 < \delta^{13}C_2 < \delta^{13}C_3 < \delta^{13}C_4$ [10]. In cases of mixing alkane gases of different genesis or sources and oxidation by microorganisms (propane bacteria), the arrangement of $\delta^{13}C$ may be confused [10–12]. The sedimentary environment controls the original carbon isotope composition of kerogen, and the carbon isotope of humic kerogen is greater than that of sapropelic kerogen [13]. Ethane has well inherited the difference of the original parent material, so that $\delta^{13}C_2$ is used as an important indicator to identify the genetic type of natural gas [14,15]. The $\delta^{13}C_2$ of alkane gas generated from sapropelic kerogen is generally lower than −29‰, and $\delta^{13}C_2$ of alkane gas generated by humic kerogen is generally higher than −28‰ [11].

Compared with crude oil, natural gas has greater molecular activity, and its migration process and migration phase state are more complex and changeable [16,17]. Natural gas can migrate not only laterally along sand bodies and nonconforming surfaces, but also vertically through faults, fractures, and pores [16,18,19]. Under formation conditions, natural gas may successively appear in one or more phases: the water-soluble phase, the oil-soluble phase, the free phase, and the diffusion phase [19–21]. Geochemical parameters, such as CH_4 content, C_1/C_2 value, stable carbon isotope, iC_4/nC_4 value, nitrogen-containing compounds and isotopes, and noble gas isotopes, are widely used in the research of natural gas migration [22–24]. During the migration of natural gas, the heavier hydrocarbon components like methane and isoalkanes will migrate preferentially over normal alkanes. Therefore, with the increase in migration distance, natural gas will have the trend of "methanation" and "isomerization" [20,25]. At the same time, isotope fractionation will also occur due to the "mass fractionation effect" and the "dissolution fractionation effect" [26].

Natural gas exploration in the Junggar Basin began in the early 1980s and made no significant breakthroughs until the discovery of the Mahe and Kelameili gas fields in the 21st century. The Basin's total proven reserve has reached 2000×10^8 m^3 [27]. According to China's 4th fourth assessment of oil and gas resources, the proportion of proven gas reserves in the lower and middle assemblages of the Junggar Basin is about 12% and 5.1% [28], respectively, which is significantly lower than other petroliferous basins [29]. In the past few years, the carbon isotopic composition and source of alkane gas in the Junggar Basin have been studied [27,30]. However, there are some problems: (i) analyzing the genesis and source of natural gas from the perspective of the whole basin will lead to some work that is not deep enough; for instance, determining from which source rocks the natural gas comes. (ii) Regional research is mainly concentrated in the basin's eastern, northwestern, and southern margins, with little research on the basin's central portion. The early proven small gas reservoirs in the eastern belt around the Penyijingxi sag of the Junggar Basin, such as the Pen 5, Mobei 2, and Mobei 5 gas reservoirs, are all secondary hydrocarbon reservoirs formed by the re-accumulation of primary oil and gas reservoirs after damage and adjustment [31,32]. The phenomenon of damage and adjustment of such primary oil and gas reservoirs also occurs in the Tarim Basin, the Sichuan Basin, the Georgina Basin, the Lower Indus Basin, and other structurally active basins [33–36].

Therefore, by analyzing the geochemical characteristics of natural gas in the eastern ring of the Penyijingxi sag, we hope to explain the genesis and source of natural gas as well as clarify the migration characteristics of natural gas after reservoir formation. This study can not only provide some important information for hydrocarbon exploration in the central part of the Junggar Basin, but also provide some ideas for natural gas research in other similar basins.

2. Geological Setting

Located between the Siberian plate, the Kazakhstan plate, and the Tarim plate, the Junggar Basin is an important part of the Central Asian orogenic belt [37]. The Junggar Basin has experienced multiple tectonic movements, such as Hercynian, Indosinian, Yanshan, and Himalayan, and has formed the current tectonic framework [38]. It can be divided into six primary tectonic units: two depressions (Ulungu and Central Depressions), three uplifts (Luliang, Western, and Eastern Uplifts), and one piedmont thrust belt (Northern Tianshan Piedmont Thrust Belt) (Figure 1a). These six primary tectonic units can be further divided into 44 secondary tectonic units. In the basin, there are three reservoir-caprock assemblages (upper, middle, and lower ones), bounded by two regional mudstone caprocks in the Lower Cretaceous Tugulu Group (including the Qingshuihe formation, Hutubihe formation, Shengjinkou formation, and Lianqinmu formation) and the Upper Triassic

Baijiantan formation [39]. Specifically, the lower assemblage mainly consists of the Permian and Carboniferous and the middle assemblage mainly consists of the Jurassic strata. In this study, the eastern belt around the Penyijingxi sag consists of the southern part of the Shixi bulge, the Mobei bulge, the western member of the Mosuowan bulge, and the eastern part of the Penyijingxi sag (Mobei Slope) (Figure 1b). The sedimentary sequence of the study area is Carboniferous, Permian, Triassic, Jurassic, Cretaceous, Paleogene, Neogene, and Quaternary (Figure 1c, the shallow stratum of the Qingshuihe formation, is not listed). The Carboniferous, Jiamuhe formation, Fengcheng formation, Lower Urho formation, Badaowan formation, and Xishanyao formation source rocks are deposited (Figure 1c) [40]. In the past few years, many commercial gas wells have been found in the study area (Figure 1b). Affected by the drilling depth, the proved natural gas in the north of the study area is mainly distributed in the Carboniferous and Jurassic; the proved natural gas in the south is mainly distributed in the Jurassic.

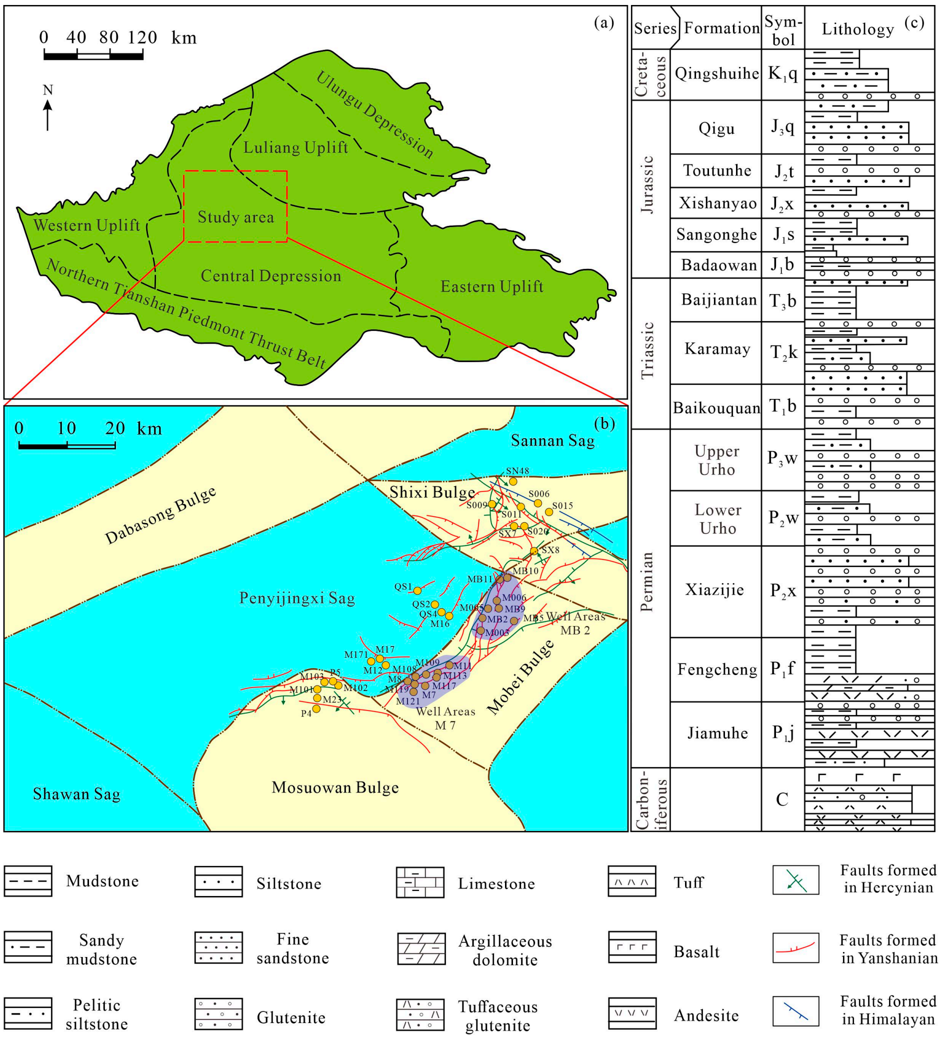

Figure 1. Geological overview of the eastern belt around the Penyijingxi sag in the Junggar Basin, NW China (modified from refs. [32,37]). (**a**) Division of tectonic units in the Junggar Basin, (**b**) geological overview of the eastern belt around Penyijingxi sag, and (**c**) stratigraphic column of the Penyijingxi sag.

3. Analytical Methods

In this study, 54 gas samples were collected from 36 wells in the eastern belt around the Penyijingxi sag for analysis of natural gas components and carbon isotopes of alkanes and light hydrocarbons (Table 1). The gas phase samples were directly collected from the wellhead using stainless steel cylinders with a diameter of 25 cm, and the gas pressure was about 2~3 MPa. After sample collection, the cylinders were placed in water to check the airtightness. The analysis and testing of the samples were completed by the Experimental Testing Research Institute of PetroChina's Xinjiang Oilfield Branch.

Table 1. Depth and source of natural gas samples.

No.	Well	Formation	Depth/m	No.	Well	Formation	Depth/m	No.	Well	Formation	Depth/m
1	M121	J1s	4222	19	QS2	J1s	3981	37	MB5	J1s	3726
2	M121	J1s	4255	20	QS4	J1s	4014	38	M108	J1s	4179
3	M109	J1s	4158	21	M101	J1s	4204	39	M109	J1s	4185
4	M113	J1s	4205	22	S006	J1s	3577	40	M11	J1s	4139
5	M115	J1s	4204	23	S006	C	4373	41	M11	J1s	4177
6	M116	J1s	4195	24	S007	C	4409	42	M7	J1s	4228
7	M117	J1s	4238	25	SX1	C	4438	43	M7	J1s	4260
8	M119	J1s	4258	26	SX1	C	4473	44	M8	J1s	4233
9	M119	J1s	4236	27	S015	J1s	nd	45	M8	J1s	4266
10	M003	J1s	3915	28	SX8	J1s	nd	46	M16	J1s	4041
11	M003	J1s	3975	29	SX14	J1s	nd	47	M171	J1s	4473
12	MB2	J1s	3921	30	MB11	J1s	3711	48	M17	J1s	4162
13	MB2	J1s	3921	31	MB2	J1s	3907	49	M12	J1s	4235
14	MB5	J1s	3726	32	M003	J1s	3972	50	M17	J1s	4192
15	MB10	J1s	3666	33	MB9	J1s	3761	51	M101	J1s	4209
16	M16	J1s	4047	34	MB9	J1s	3778	52	M102	J1s	4251
17	QS1	J1s	3945	35	M005	J1s	3890	53	M103	J1s	4251
18	QS1	J1s	3945	36	M006	J1s	3759	54	P5	J1s	4250

Notes: J1s means Jurassic Sangonghe formation, C means Carboniferous, nd means no data, M means Mo, MB means Mobei, QS means Qianshao, SX means Shixi, P means Pen.

3.1. Components of the Natural Gas

The composition (methane-pentane) of natural gas was analyzed by an Agilent 7890A gas chromatograph. The sample pretreatment and test process refer to the standard of natural gas composition analysis of the People's Republic of China (GB/T 13610-2020). Before each experiment, we carried out two or more consecutive standard gas injection checks to control the difference between the response values of each component within 1%. Therefore, the experimental results are reliable. The instrument was equipped with two thermal conductivity detectors and one flame ionization detector. In the experiment, a constant-temperature heating furnace was used to keep the sample temperature around 75 °C and make the sample composition uniform. High-purity (99.999%) helium was used as the carrier gas, with a flow rate of 2 mL/min. The outlet pressure of the cylinder was controlled at 0.2 MPa and the air flow rate at 80 mL/min. The split ratio was controlled at 150:1. DB-1 chromatographic columns were used in the experiment. The initial temperature of the chromatographic column box was 40 °C (for 2 min), and then the temperature rose to 90 °C at a rate of 10 °C/min, and then to 200 °C at a rate of 5 °C/min (for 5 min). Finally, the composition of the test sample was determined by the retention time of the standard gas.

3.2. Natural Gas Light Hydrocarbon

The Agilent 6890B gas chromatograph was used for light hydrocarbon (pentane-octane) analysis of natural gas. The sample pretreatment and experimental process refer to the oil and natural gas industry standard of the People's Republic of China for stable light component analysis (SY/T 0542-2008). The instrument was also equipped with a thermal conductivity detector and a flame ionization detector. The constant temperature furnace was also used to heat the sample in the experiment. High-purity (99.999%) helium was used as the carrier gas with a flow rate of 1 mL/min. The outlet pressure of the cylinder was controlled at 0.2 MPa and the air flow rate at 80 mL/min. The split ratio was controlled at 150:1. Pona chromatographic columns were used in the experiment. The initial temperature of the chromatographic column box was 30 °C (for 15 min), and then the temperature was raised to 70 °C at a rate of 3 °C/min, and then to 300 °C (for 10 min) at a rate of 3 °C/min. As in Section 3.1, the composition of the test sample was determined by the retention time of the standard gas. Each sample was measured repeatedly to ensure that the difference between the two measurement results was not greater than the precision specified in the standard. Then, the arithmetic mean of the two measurement results was used as the analysis result. Therefore, the experimental results are reliable.

3.3. Carbon Isotopic Composition of the Natural Gas

The carbon isotope analysis of natural gas was completed on the Delta V Advantage isotope mass spectrometer connected with the Agilent 7890A gas chromatograph. The sample pretreatment and experimental process refer to the organic geochemical analysis standard of geological samples of the People's Republic of China (GB/T 18340.2-2010). First, the components of natural gas were separated using an Agilent 7890A gas chromatograph (the experiment used an HP-5MS column). Then, the hydrocarbon gas was sent into the isotope mass spectrometry oxidation furnace to be converted into CO_2. Finally, CO_2 was introduced into the Delta V Advantage isotope mass spectrometer to determine the carbon isotope composition. The initial temperature of the chromatographic column box was 40 °C (for 5 min), and then it rose to 200 °C (for 18 min) at 10 °C/min. The experiment used high-purity (99.999%) helium as the carrier gas at a flow rate of 2 mL/min. The split ratio of the methane carbon isotope analysis was 50:1 and the split ratio of the ethane-pentane isotope analysis was 10:1. The standard samples for experimental analysis were obtained from the national standard material sharing platform of China. The experimental results are based on the VPDB standard. The precision of the carbon isotope determination meets the requirements that the repeatability value (r) is lower than 0.4 and the reproducibility value (R) is lower than 0.5, which can be considered reliable.

4. Results

4.1. Components of the Natural Gas

The natural gas in the eastern belt around the Penyijingxi sag is absolutely dominated by alkane gases. The volume fraction of methane varies from 71.36% to 93.34%, with an average of 87.94% (Table 2). Natural gas has a dryness coefficient ranging from 0.76 to 0.95, averaging 0.91, and is dominated by wet gas. The wide range of its dryness coefficient indicates that the natural gas may be generated by source rocks at different stages of thermal evolution. The non-hydrocarbons in natural gas are mainly N_2 (volume fraction: 0.69–11.95%, with an average of 2.56%) and CO_2 (volume fraction: 0–1.49%, with an average of 0.45%). The gas composition varies among the zones: the gas in the Shixi bulge has a relatively low content of CH_4, with an average of less than 80%, and a relatively high content of N_2, averaging 6.75%. The gas in the Mobei bulge, Mobei Slope, and Mosuowan bulge has a relatively high content of CH_4, with an average greater than 87.58%, and a relatively low content of N_2, averaging less than 3.0% (Table 2).

Table 2. Natural gas compositions by zone in the eastern belt around the Penyijingxi sag, Junggar Basin.

Category	Carboniferous	Jurassic Sangonghe Formation			
	Shixi Bulge	**Shixi Bulge**	**Mobei Bulge**	**Mobei Slope**	**Mosuowan Bulge**
CH_4/%	71.36~88.82	75.10~91.12	84.56~93.34	73.88~91.20	87.49~89.51
	79.10	81.42	89.97	87.58	88.31
C_2H_6/%	3.70~7.92	4.38~9.11	3.10~6.69	4.02~10.90	4.25~4.70
	5.87	7.39	4.25	5.37	4.5
C_3H_8/%	1.07~4.36	1.47~4.72	0.93~3.01	1.07~5.96	1.47~1.98
	3.28	3.30	1.50	2.20	1.76

Table 2. *Cont.*

Category	Carboniferous	Jurassic Sangonghe Formation			
	Shixi Bulge	Shixi Bulge	Mobei Bulge	Mobei Slope	Mosuowan Bulge
$C_4H_{10}/\%$	1.08~4.55	0.90~4.04	0.50~1.95	0.60~4.38	0.84~1.43
	3.32	2.59	0.98	1.45	1.15
$C_5H_{12}/\%$	0.54~1.78	0.33~1.49	0.08~0.93	0.24~1.57	0.24~0.62
	1.32	1.00	0.36	0.54	0.45
$CO_2/\%$	0.00~0.37	0.63~1.07	0~1.49	0.31~0.70	0.41~0.62
	0.17	0.80	0.40	0.52	0.54
$C_1/C_{1\text{-}5}$	0.82~0.93	0.80~0.93	0.87~0.95	0.76~0.94	0.91~0.93
	0.85	0.8	0.93	0.90	0.92

Note : $\frac{71.36\sim88.82}{79.10(4)} = \frac{\text{Min}\sim\text{Max}}{\text{Ave}}$, see Appendix A for all data.

4.2. Carbon Isotopic Composition of the Natural Gas

The carbon isotopic compositions of the components of the natural gas in the eastern belt around the Penyijingxi sag were analyzed. The carbon isotope ratio of methane ($\delta^{13}C_1$) ranges from −45.57‰ to −31.19‰, with an average of −37.48‰, showing a single peak mainly within the range from −42.5‰ to −35.0‰ (Figure 2a). The carbon isotope ratio of ethane ($\delta^{13}C_2$) ranges from −31.69‰ to −24.66‰, with an average of −27.62‰. Similar to $\delta^{13}C_1$, it shows a single peak mainly within the interval from −35.0‰ to −27.5‰ (Figure 2b). The carbon isotope ratio of methane ($\delta^{13}C_3$) ranges from −28.76‰ to −23.56‰, with an average of −26.27‰, showing a single peak mainly within the range from −27.5‰ to −24.5‰ (Figure 2c). The carbon isotope ratio of methane ($\delta^{13}C_4$) ranges from −27.96‰ to −23.64‰, with an average of −26.41‰, showing a single peak mainly within the range from −26.5‰ to −24.5‰ (Figure 2d).

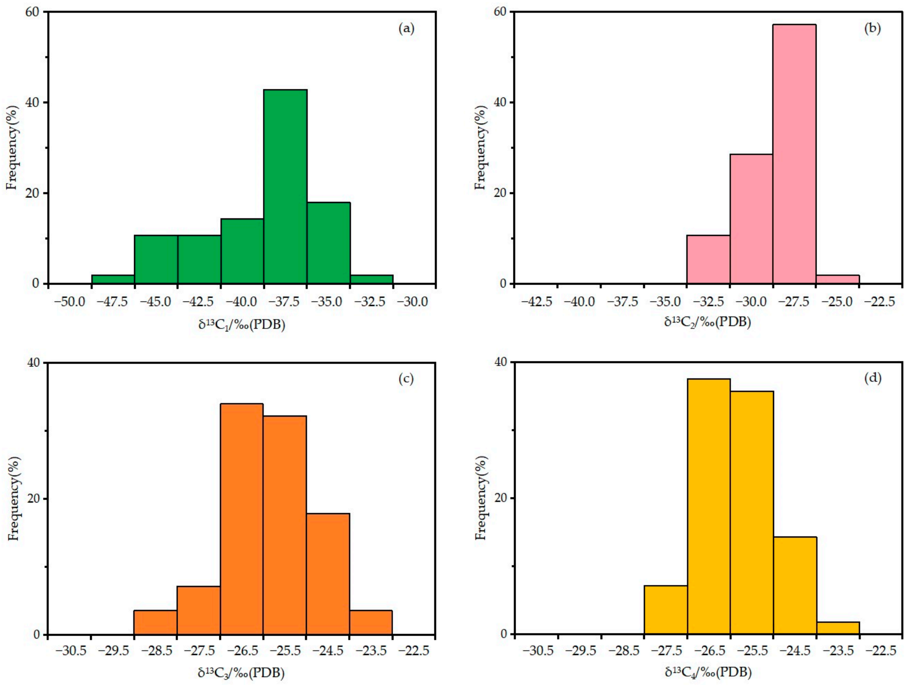

Figure 2. Histogram of $\delta^{13}C_1$ (**a**), $\delta^{13}C_2$ (**b**), $\delta^{13}C_3$ (**c**), and $\delta^{13}C_4$ (**d**) of the natural gas in the eastern belt around the Penyijingxi sag, Junggar Basin.

Due to their reversed isotope kinetic fractionation pattern, the $\delta^{13}C$ of the natural gas of organic origin increases gradually with the carbon number, forming a positive carbon isotopic series, while the $\delta^{13}C$ of the natural gas of inorganic origin forms a negative carbon isotopic series [9,10]. Gas samples with positive carbon isotopic series account for 41.38% of all the samples collected from the studied area. The remaining samples are all slightly and partially isotopically reversed, with the carbon isotopic series as $\delta^{13}C_1 < \delta^{13}C_2 < \delta^{13}C_3 < \delta^{13}C_4$ (Figure 3). The causes for carbon isotopic reversal include: (i) mixing of organic and inorganic alkane gases, (ii) mixing of coal- and oil-associated gases, (iii) microbial oxidation, and (iv) mixing of same-type alkane gases of different sources or same-source alkane gases of different periods [11,41]. In the studied area, natural gas reservoirs are generally located 3500 m below the surface or deeper. According to a geothermal gradient of 25°C/km [42], the reservoir temperature should be higher than 87.5°C, making it impossible for propane oxidizing bacteria to survive [43]. Therefore, we can exclude microbial oxidation from the causes. Other possible causes for carbon isotopic reversal are discussed below.

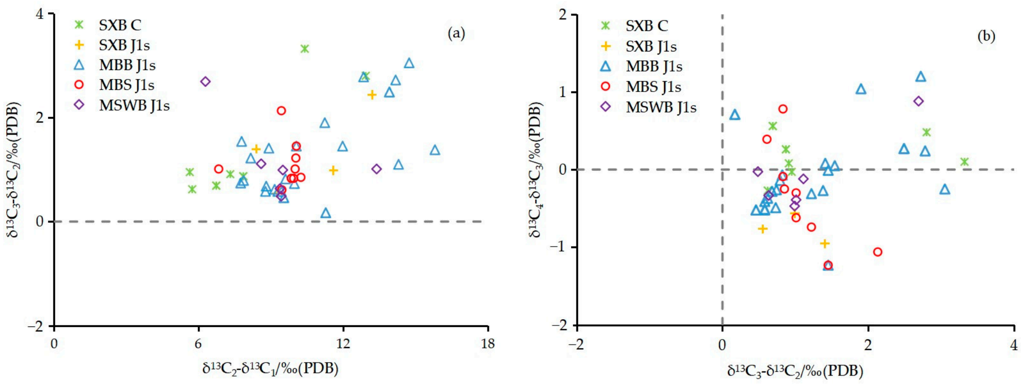

Figure 3. Cross-plots of $\delta^{13}C_2$-$\delta^{13}C_1$ vs. $\delta^{13}C_3$-$\delta^{13}C_2$ (**a**) and $\delta^{13}C_3$-$\delta^{13}C_2$ vs. $\delta^{13}C_4$-$\delta^{13}C_3$ (**b**) of the natural gas in the eastern belt around the Penyijingxi sag, Junggar Basin. SXB C means the Carboniferous system of Shixi bulge, SXB J1s means Jurassic Sangonghe formation of Shixi bulge, MBB J1s means Jurassic Sangonghe formation of Mobei bulge, MBS J1s means Jurassic Sangonghe formation of Mobei slope, MSWB J1s means Jurassic Sangonghe formation of Mosuowan bulge.

5. Discussion

5.1. Genesis Types of the Natural Gas

The carbon isotopic compositions of methane and ethane and the carbon isotopic series of their homologues are important indicators to identify whether the alkane gases are of inorganic or organic origin, and are commonly used to determine the genesis of natural gas [7]. The alkane gases in the natural gases from the Shixi, Mobei, and Mosuowan bulges and the Mobei slope have a positive carbon isotopic series ($\delta^{13}C_1 < \delta^{13}C_2 < \delta^{13}C_3$) that is reversed for butane (Figure 3). This partial reversal may be due to the mixing of natural gases of different genesis, migration, or secondary changes [11,12]. Primary alkane gases should have a positive carbon isotopic series ($\delta^{13}C_1 < \delta C^{13}{}_2 < \delta^{13}C_3 < \delta^{13}C_4$). In addition, while the isotopic composition of methane of inorganic origin is generally greater than −30‰, this value of the gases in the studied area is less than −30‰ (Figure 4). Therefore, it can be concluded that the natural gases in the eastern belt around the Penyijingxi sag are of organic origin, and that the reversed isotopic series of alkane gases should not be caused by the mixing of organic and inorganic alkane gases.

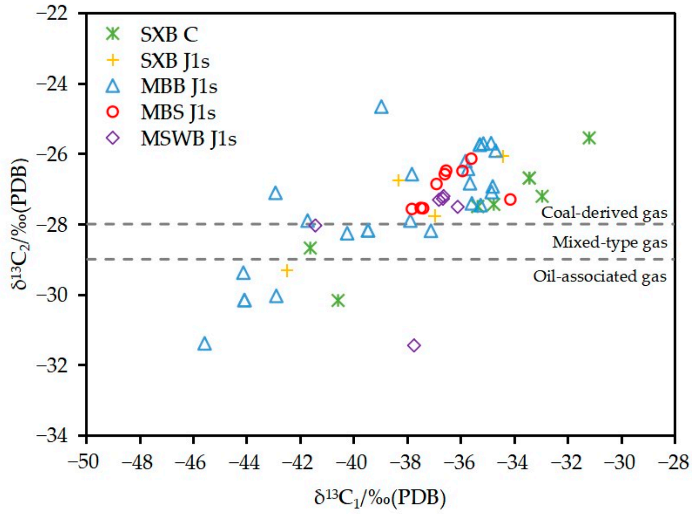

Figure 4. Genetic types identification chart for natural gases in the eastern belt around the Penyijingxi sag, Junggar Basin based on $\delta^{13}C_2$ & $\delta^{13}C_1$ (plate from ref. [11]).

The $\delta^{13}C_2$ value of alkane gases is a feature basically inherited from the parent material and is less influenced by the maturity of the source rocks. It is usually used as an important indicator for gas genesis identification [14,15]. In this paper, we identify gases with $\delta^{13}C_2 > -28‰$ as coal-derived gas, gases with $\delta^{13}C_2 < -29‰$ as oil-associated gas, and gases with $\delta^{13}C_2$ between −28‰ to −29‰ as mixed-type gas (Figure 4) [11]. The samples from the Shixi, Mobei, and Mosuowan bulges are distributed in all three intervals (Figure 4) but are mainly coal-derived gases. Only a few samples are oil-associated or mixed-type gas, which are the thermal degradation products of sapropelic-type and humic-type kerogens. The samples from the Mobei slope all fall in the coal-derived gas interval, which is generated by humic kerogen. Obviously, different from those in the Shixi, Mobei, and Mosuowan bulges, the Jurassic reservoir of the Mobei Slope only produces coal-derived gas. As revealed by the period analysis of the faults in the studied area, both the Hercynian and Yanshanian faults developed in the bulge zone, while only the Yanshanian faults developed in the slope zone [32]. This difference in vertical migration channels may result in the different gas types in bulge and slope zones.

Light hydrocarbons are important components of both natural gas and crude oil. Their variety becomes much wider as the number of carbon atoms increases, and their boiling points do not exceed 200°C in general. In natural gas genesis identification, indicators related to liquid and light C_5~C_8 hydrocarbons are commonly used for comparing the natural gases' type, maturity, and source [44]. The indicators for identifying organic matter type include the relative content of dimethyl cyclopentane (ΣDMCH) of various structures, n-heptane (nC_7), methylcyclohexane (MCH) in C_7 light hydrocarbons as well as the relative content of cycloalkanes, n-alkanes, and isomeric alkanes in $C_{5\sim7}$ hydrocarbons [45]. MCH, mainly from higher plants' lignin, cellulose, sugar, etc., has relatively stable thermodynamic properties and is a good parameter to indicate the type of terrestrial parent material. Its abundance is an important characteristic of light hydrocarbons in coal-derived gas. ΣDMCH, mainly from the lipid compounds of aquatic organisms, is affected by maturity. The high content of ΣDMCH indicates oil-associated gas. nC_7, mainly from algae and bacteria, is a good maturity indicator [46]. In the C_7 light hydrocarbons from the gases in the studied area, the relative content of MCH ranges from 29.38% to 53.35%, with an average of 41.98% (Figure 5). The relative content of ΣDMCH ranges between 4.63% and 45.79%, with an average of 14.30%. The high relative content of MCH and low relative content of ΣDMCH indicate that the natural gases in the studied area are mainly from type III (humic) kerogen and are dominated by coal-derived gas. This conclusion is consistent with the results of the alkane carbon isotopic analysis above.

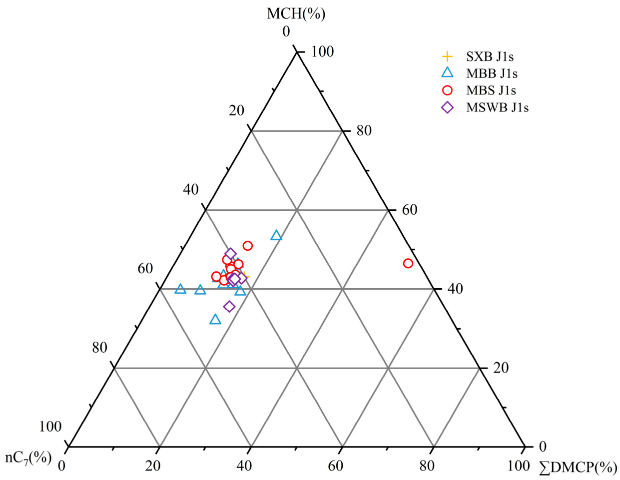

Figure 5. Characteristics of C_7 light hydrocarbons from natural gases in the eastern belt around the Penyijingxi sag, Junggar Basin.

5.2. Sources of Natural Gas

In the studied area, adjacent to the hydrocarbon-rich Penyijingxi sag in the Central Depression of the Junggar Basin, multiple sets of potential Carboniferous, Permian, and Jurassic source rocks have been developed (Table 3). According to the geochemical evaluation method of terrigenous source rocks (SY/T 5735-1995), the Carboniferous source rocks are of medium-poor quality, primarily composed of type III kerogen, and are mainly gas-producing. The Jiamuhe formation, Lower Urho formation, and Jurassic source rocks are of medium-good quality, composed of type III kerogen, and are mainly gas-producing. The Fengcheng formation source rocks are of good quality, composed of type II kerogen, and are mainly oil-producing. According to the 4th resource evaluation of the Junggar Basin, the total gas generation intensity of the source rocks in the Penyijingxi sag is 8000×10^6~$13{,}000 \times 10^6$ m^3/km^3 [28], which indicates that the above-mentioned source rocks have generated a large amount of natural gas and can provide sufficient gas to fill the eastern belt around the sag.

Table 3. Geochemical characteristics of the main source rocks in the Penyijingxi sag, Junggar Basin [47,48].

Stratum	TOC/%	$(S_1 + S_2)$/(mg/g)	Chloroform Bitume "A"/%	Hydrogen Index/(mg/g.TOC)	Kerogen Type
J2x	0.40~5.87	0.05~17.70	0.016~0.918	/	III
	1.42	2.03	0.267	/	
J1b	0.42~5.86	0.08~29.67	0.025~4.916	/	III
	1.68	3.03	0.555	/	
P2w	0.18~14.03	0.01~37.52	0.0007~0.8024	1.20~950.00	III
	1.69	2.06	0.0692	74.16	
P1f	0.03~4.43	0.1~59.84	0.0004~1.8933	3.33~1872.37	II
	0.93	4.66	0.2507	306.54	
P1j	0.1~14.04	0.01~17.60	0.0025~0.4539	1.64~507.89	III
	2.38	1.81	0.052	55.85	
C	0.03~19.8	0.01~37.52	0.001~0.3515	1.63~365.06	III
	1.63	0.84	0.031	52.45	

Note : $\frac{0.40\sim5.87}{1.42} = \frac{\text{Min}\sim\text{Max}}{\text{Ave}}$.

The Jurassic coal-bearing source rocks have high organic matter abundance and great hydrocarbon generation potential, but the vitrinite reflectance (Ro) is as low as 0.5% to 0.7% [40]. These source rocks enter their early gas generation stage only when their Ro is greater than 0.8% [49]. Therefore, the Jurassic source rocks are not the main hydrocarbon source for natural gases in the studied area. The Permian Fengcheng formation (P_1f) is a residual sea-lagoon deposit of a sea–land transition environment with type II kerogen (Table 3). It is in the mature-highly mature stage [48]. Given the results of the ethane carbon isotopic analysis above, it should be the source of oil-associated gas in the middle and lower assemblages of the eastern belt around the Penyijingxi sag. The Carboniferous, Jiamuhe, and Lower Urho formations contain abundant organic matter, have an average TOC value greater than 1.5% (Table 3), and are dominated by type III kerogen. Meanwhile, they are in the mature-highly mature stage [40]. According to the relationship between the hydrocarbon generation stage and the Ro value of source rocks [47], these three sets of gas-prone source rocks are at the peak of gas generation, and all of them could be the potential gas sources for the coal-derived gases in the studied area.

Mango has proposed the theory of light hydrocarbon generation based on the light hydrocarbon data of more than 2000 different types of crude oil and the steady-state catalytic kinetic model of heptane genesis [44,50]. According to his theory, all light hydrocarbons generated from the same source rocks have similar K_1 values (Equation (1)) and K_2 values (Equation (2)), which are related to their parent material, but not to the maturity.

$$K_1 = A_1/A_2 \tag{1}$$

where A_1 = 2-MH + 2,3-DMP and A_2 = 3-MH + 2,4-DMP. 2-MH means 2-methylhexane, 2,3-DMP means 2,3-dimethylpentane, 3-MH means 3-methylhexane, and 2,4-DMP means 2,4-dimethylpentane.

$$K_2 = P_3/(P_2 + N_2) \tag{2}$$

where P_2 = 2-MH + 3-MH, P_3 = 2,2-DMP + 2,4-DMP + 2,3-DMP + 3,3-DMP + 3-EP, and N_2 = *cis*-1,3-DMCP + *trans*-1,3-DMCP + 1,1-DMCP. 2,2-DMP means 2,2-dimethylpentane, 3,3-DMP means 3,3-dimethylpentane, 3-EP means 3-ethylpentane, cis-1,3-DMCP means cis-1,3-dimethylcyclopentane, and trans-1,3-DMC means trans-1,3-dimethylcyclopentane.

The K_1 values of the light hydrocarbons associated with the natural gas in the studied area are distributed along two different trend lines (Figure 6a) and are well correlated. The average K_1 values of the black trend line and the orange trend line (0.63 vs. 1.29) are significantly different, indicating two different sources of natural gas in the studied area. In the cross-plot of the K_1 vs. K_2 values, natural gas from different sources will be distributed in different regions [50]. The gas samples collected from the studied area are distributed in two areas: the oil-associated gas area on the left, represented by Well Mobei 2 (with $\delta^{13}C_2$ as −29.38‰) and the coal-derived gas area on the right, represented by Well Qianshao 1 (with $\delta^{13}C_2$ as −27.55‰) (Figure 6b). This pattern further indicates that the gas in the studied area should come from one set of sapropelic source rocks and one set of humic source rocks separately. To further determine the source of the coal-derived gas, the geochemical characteristics of light hydrocarbons from the natural gas in the studied area and from crude oil were compared.

By comparing biomarker compounds, Wu (2012) identified that the Cretaceous crude oil produced from the well Shixi 10 located in the Shixi bulge is from the Lower Urho formation [51]. In addition, he selected seven light hydrocarbons, such as *trans*-1,3-DMP/*trans*-1,2-DMP, from crude oil and determined their fingerprint features (Figure 7). By comparing the light hydrocarbons associated with natural gas in the studied area with the light hydrocarbons associated with crude oil from the Lower Urho formation source rocks, we find that the fingerprint features of the light hydrocarbons associated with natural gas in the Shixi bulge, Mobei bulge, Mobei slope, and Mosuowan bulge are highly similar to those of the above-mentioned crude oil-associated light hydrocarbons (Figure 7). Therefore, it can be inferred that the Lower Urho formation of the Penyijingxi sag should be the main source rock for the coal-derived gas in the studied area.

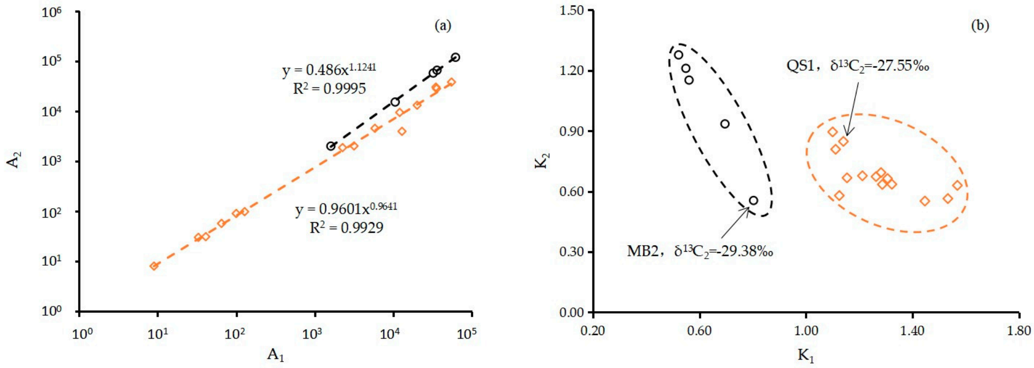

Figure 6. Cross-plots of A_1 vs. A_2 (**a**) and K_1 vs. K_2 (**b**) for the light hydrocarbons associated with the natural gas in the Eastern belt around the Penyijingxi sag, Junggar Basin (Plate from ref. [50]).

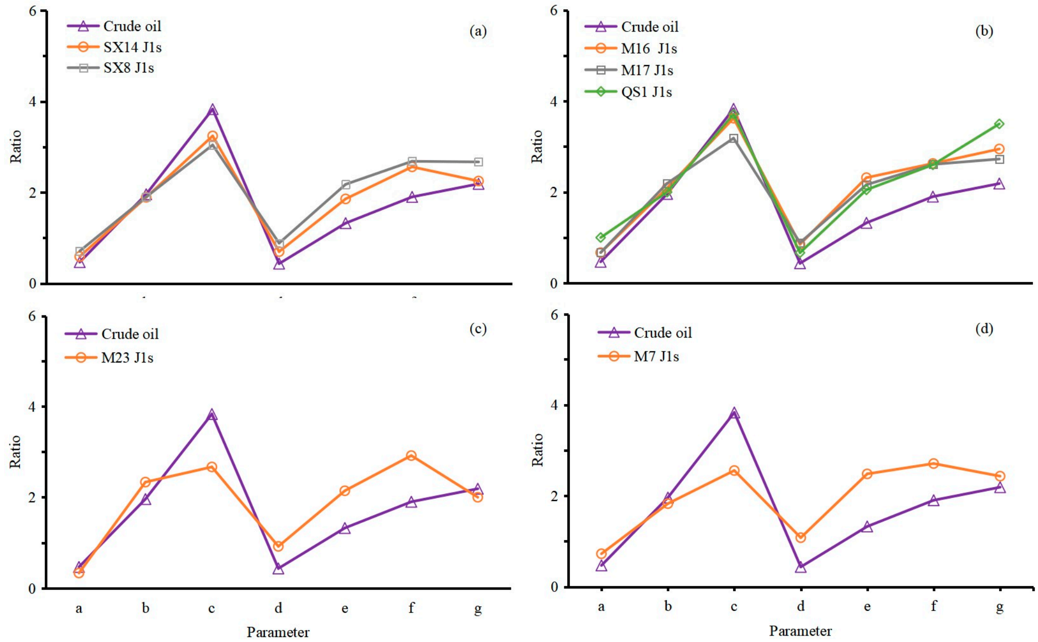

Figure 7. Fingerprint characteristics of light hydrocarbons associated with the natural gas in the eastern belt around the Penyijingxi sag, Junggar Basin and the crude oil (crude oil data from ref. [51]). a. *trans*-1,3-DMP/*trans*-1,2-DMP, b. CH/MCH, c. MCH/∑DMCH, d. n-heptane/(ECH + MCH), e. n-hexane/CH, f. 3-MP/3-MP, and g. 3-MH/2,3-DMP. (**a**) Shixi bulge, (**b**) Mobei Slope, (**c**) Mosuowan bulge, and (**d**) Mobei bulge. trans-1,3-DMP means 1-trans 3-dimethylpentane, trans-1,2-DMP means 1 trans 2-dimethylpentane, CH means cyclohexan, MCH means methylcyclohexane, ΣDMCH means Σdimethyl cyclohexane, ECH means ethylcyclohexane, 2-MP means 2-methylpentane, 3-MP means 3-methylpentane, 3-MH means 3-methylhexane, 2,3-DMP means 2,3-dimethylpentane.

The good linear relationship between the alkane gases' $\delta^{13}C_1$ and the Ro value of their source rocks, with carbon isotopes becoming heavier with thermal evolution, is useful for gas source comparison [14]. Many researchers have fitted the $\delta^{13}C$-Ro regression equations for coal-derived and oil-associated gases [52,53]. Considering the regional geochemical characteristics, we used the empirical regression Equations (3) and (4) proposed by Chen et al. (2021) to calculate the maturity degree of the source rocks of the natural gas. The results show (Table 4) that the Ro value of the oil-associated gas is between 0.75% to 1.55%, and the Ro value of the coal-derived gas is between 0.61% to 1.36%. As a result, it is assumed that oil-associated gas and coal-derived gas originate in the mature to highly mature stage from the source rocks of the Fengcheng formation and Lower Urho formation, respectively. This conclusion is consistent with the measured Ro values of the source rocks of the Fengcheng and Lower Urho formations [40,49]. The ratio of the methane carbon isotope in the alkane gases varies widely from −45.57‰ to −31.19‰ (Figure 4), indicating that natural gases are products of source rocks at different stages of thermal evolution. This conclusion is consistent with the results based on the dryness coefficient.

$$\text{Coal} - \text{derived gas}: \ \delta^{13}C_1 = 25\lg Ro - 37.5 \quad (3)$$

$$\text{Oil} - \text{associated gas}: \ \delta^{13}C_1 = 25\lg Ro - 42.5 \quad (4)$$

Table 4. Maturity degrees of natural gases in the eastern belt around the Penyijingxi sag, Junggar Basin.

Category		Carboniferous	Jurassic Sangonghe Formation			
		Shixi Bulge	Shixi Bulge	Mobei Bulge	Mobei Slope	Mosuowan Bulge
Oil-associated	$\delta^{13}C_1$-$\delta^{13}C_2$/‰	−10.41	−13.19	−14.72~−12.85	/	−13.19
	Ro/%	1.19	1.00	0.75~0.96	/	1.55
Coal-derived	$\delta^{13}C_1$-$\delta^{13}C_2$/‰	−7.86~−5.64	−11.59~−8.38	−15.81~−7.75	−10.25~−6.84	−10.2~−8.15
	Ro/%	1.22~1.79	0.93~1.33	0.61~1.30	0.97~1.36	1.01~1.21

5.3. Gas Migration and Accumulation

With longer migration distances, the alkane gas' $\delta^{13}C_1$ value will decrease and the C_1/C_2 ratio will increase. Therefore, they are highly sensitive geochemical parameters representing the migration characteristics of natural gas [25]. Furthermore, when the gas has undergone no or only weak secondary alteration processes, the differences in its components and carbon isotope compositions are mainly influenced by the maturity of the source rocks, with both $\delta^{13}C_1$-$\delta^{13}C_2$ and Ln(C_1/C_2) increasing with the maturity of the source rocks. On the contrary, when the gas has been subject to diffusion, migration, and dispersion, its $\delta^{13}C_1$-$\delta^{13}C_2$ will gradually increase and its Ln(C_1/C_2) will decrease [54]. During the Neogene-Quaternary period, the southern margin of the Junggar Basin tilted extensively, not only causing the disappearance of the Chepaizi-Mosuowan Paleo-uplift, but also making the central Junggar Basin a southward-tilted monocline [55]. As a result, hydrocarbons migrated and adjusted inevitably. Was there a large-scale lateral gas migration from south to north in the middle and lower assemblages in the eastern belt around the Penyijingxi sag during this period? We collected gas samples from adjacent wells of the same members within the Mobei Bulge for a comparative study.

At present, the proven gas reserves of both well areas M 7 (Mo 7) and MB 2 (Mobei 2) in the Mobei Bulge are concentrated in the Jurassic Sangonghe formation (Figure 1b). Although close to each other, the two well areas have significantly different gas components and carbon isotopic compositions. The average $\delta^{13}C_1$ and $\delta^{13}C_2$ of the gas in well area M 7 are −35.85‰ and −26.11‰, respectively, while the average of $\delta^{13}C_1$ and $\delta^{13}C_2$ of the gas in well area MB 2 are −40.05‰ and −28.39‰, respectively. These data indicate that the source rocks for the gas in well area M 7 are more mature than those for the gas in well area MB 2. Eight typical wells were selected in the well areas M 7 and MB 2 to compare gas migration parameters (Figure 8). It was found that the $\delta^{13}C_1$ of the alkane gas and especially the single hydrocarbon component C_1/C_2 ratio tend to decrease from south to north in the Mobei bulge. If the lightening of alkane gas $\delta^{13}C_1$ is caused by the long-distance lateral migration of gas, then the C_1/C_2 ratio should be increasing rather than decreasing. Taking into account the maturity analysis of the gases in the well areas M 7 and MB 2 above, the difference in the gas components and carbon isotopic compositions between adjacent well areas in the eastern belt around the Penyijingxi sag should be caused by the varied maturity of the source rocks rather than the lateral migration of gas. In other words, there was no significant lateral gas migration due to tilting.

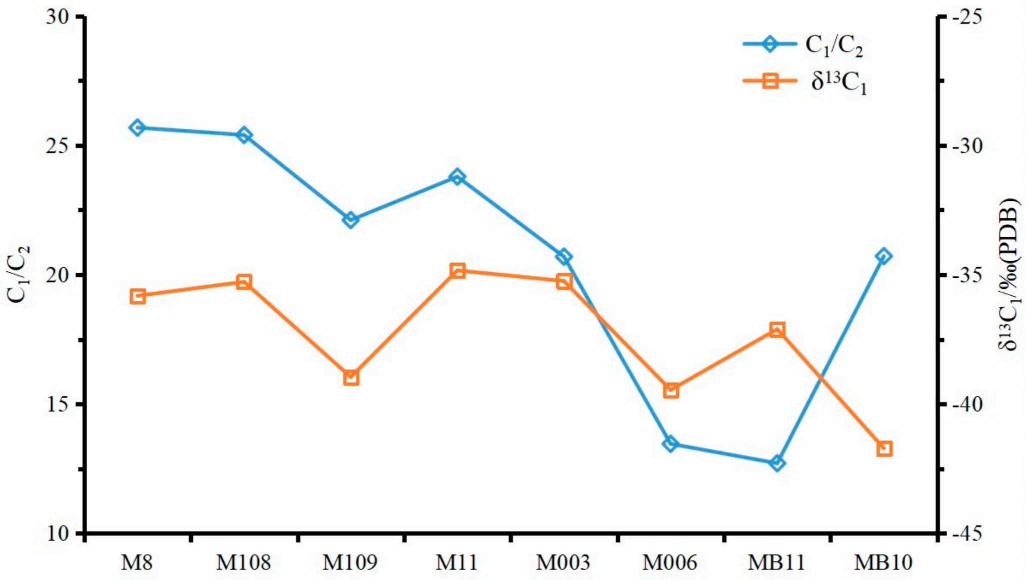

Figure 8. Geochemical parameters of the Mobei bulge in the eastern belt around the Penyijingxi sag, Junggar Basin.

Did large-scale gas migration occur between the superimposed gas-bearing formations in the eastern belt around the Penyijingxi sag? We explored this problem by conducting a case study of the typical well pen 4 (P 4) in the Mosuowan bulge (Figure 1b). From deep to shallow strata, coal-derived, mixed-type, and oil-associated gases appear successively in well pen 4, with the carbon isotopic series changing from reversed ones to positive ones (Figure 9). The maturity of the natural gas source rocks is obtained using regression Equations (3) and (4): the oil-associated gases with Ro values ranging from 1.42% to 1.55% and the coal-derived gases with Ro values ranging from 0.95% to 1.05%. The alkane gases from reservoirs at depths of 4676.00 m and 4514.00 m in well pen 4 are mixed-type gases (Figure 9a) with reversed carbon isotopic series (Figure 9b), and should be a mixture of late filled low-maturity (at a depth of 4514.00 m, with alkane gas $\delta^{13}C_1$ as -43.88‰) to mature (at a depth of 4676.00 m, with alkane gas $\delta^{13}C_1$ as -37.99‰) coal-derived gas and early filled highly matured oil-associated gas. The alkane gases from reservoirs at depths of 5032.45 m and 5100.57 m in well pen 4 are coal-derived gases (Figure 10a), but they also have a reversed carbon isotopic series. The results of the gas source and maturity analyses indicate it is caused by the mixing of the gases of the same genetic type formed at different stages. This conclusion is consistent with the view proposed by Zou et al. (2005) that hydrocarbons are continuously filling the Jurassic system of the central Junggar Basin [33]. The analysis above shows that gases from the upper and lower gas reservoirs of well pen 4 are mixed. Further, it is reasonable to infer that there is vertical gas migration in the studied area, and that the reversed carbon isotopic series of the mixed-type and coal-derived gases are caused by the mixing of coal-derived and oil-associated gases and the mixing of alkane gases of the same genetic type that formed at different stages, respectively.

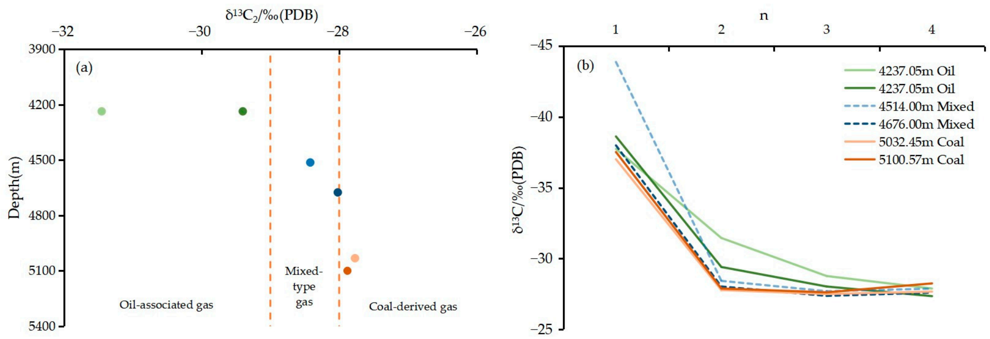

Figure 9. Relationship of $\delta^{13}C_2$ vs. depth (**a**) and carbon isotopic compositions of alkanes (**b**) of the natural gases from well pen 4 in the Mosuowan Bulge, Junggar Basin (data from ref. [56]).

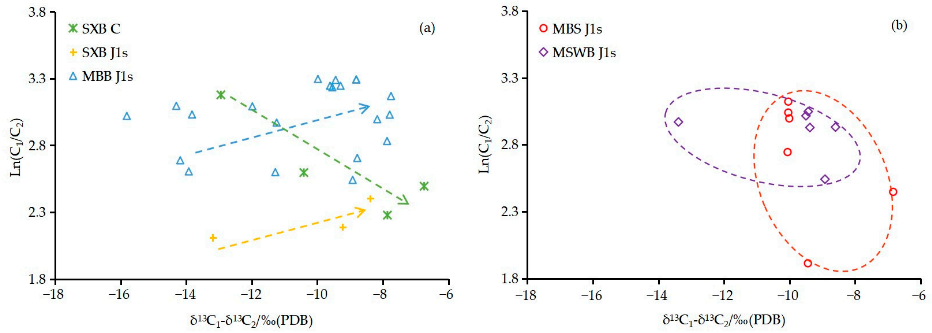

Figure 10. Relationship of $\delta^{13}C_1$-$\delta^{13}C_2$ vs. Ln(C_1/C_2) in the eastern belt around the Penyijingxi sag, Junggar Basin (Plate from ref. [54]).

The $\delta^{13}C_1$-$\delta^{13}C_2$ and Ln(C_1/C_2) of the gases from the Sangonghe formation of the Shixi Bulge and the Sangonghe formation of the Mobei Bulge in the studied area increase synchronously, reflecting the change of gas parameters with maturity (Figure 10a). The data about the gases from the Sangonghe formation of the Mobei Slope and Mosuowan Bulge show no regular pattern (Figure 10b), preventing us from determining the main controlling factors for the differences in their components and carbon isotopic compositions. The carboniferous gases in the Shixi Bulge have gradually increasing $\delta^{13}C_1$-$\delta^{13}C_2$ and gradually decreasing Ln(C_1/C_2), showing obvious characteristics of residual gases after diffusion migration (Figure 10a). In addition, the gas–oil ratio of the reservoir decreases from 4794.59 m^3/t to 204.86 m^3/t along the direction indicated by the green arrow in Figure 10, further confirming the previous diffusion migration of Carboniferous gases, as the gas–oil ratio only decreases due to the loss of lighter components after oil and gas accumulation [57]. Diffusion migration is an important method of forming gas pools in sedimentary basins [25], therefore we speculated that there may be gas pools formed by diffusion migration of carboniferous natural gas in the shallow layers. Through a comprehensive analysis of natural gas composition, carbon isotope, and light hydrocarbon fingerprint parameters, this study explains the genesis and source of natural gas, as well as clarifies the migration characteristics of natural gas after reservoir formation. We can conclude that the gases in the middle and lower assemblages of the eastern belt around the Penyijingxi sag were mainly produced in the processes where hydrocarbons were generated by the source rocks of the Lower Urho and Fengcheng formations and then migrated along faults under greater pressure to fill the near (Carboniferous) or distant (Jurassic Sangonghe formation) reservoirs. The Yanshanian faults only cut through the Triassic–Jurassic systems, resulting in only coal-derived gas production in the slope zone. The Hercynian faults cut through the Carboniferous–Triassic systems and "relay" gases with the Yanshanian faults, enabling the bulge areas to produce coal-derived, oil-associated, and mixed-type gases. The tilting during Himalayan movements did not cause significant lateral migration of the gases in the Sangonghe formation, while diffusion migration of the

Carboniferous gases occurred after reservoir formation. We believe that: (i) the shallow layer (e.g., the Cretaceous) can be considered one of the key strata series for searching for secondary hydrocarbon reservoirs in the next stage of hydrocarbon exploration and (ii) the geochemical parameters and analysis process used in this paper have certain reference values for studying the origin of natural gas in similar petroliferous basins (e.g., the Tarim Basin and the Georgina Basin).

6. Conclusions

The natural gases in the middle and lower assemblages of the eastern belt around the Penyijingxi sag, Junggar Basin consist of a high percentage of methane (71.36–93.34%) with the dryness coefficient ranging from 0.76 to 0.95, averaging 0.91. There are also varying amounts of non-hydrocarbons, such as CO_2 (<1.49%) and N_2 (0.69–11.95%). The carbon isotopic composition of methane ($\delta^{13}C_1$) ranges widely from −45.57‰ to −31.19‰, indicating that the natural gases may be products of source rocks at different stages of thermal maturity.

The contained alkanes show an overall carbon isotopic composition trend as $\delta^{13}C_1 < \delta^{13}C_2 < \delta^{13}C_3 < \delta^{13}C_4$ and have $\delta^{13}C_1$ values < −30‰, indicating that the natural gases are of organic origin. The methane and ethane isotopic compositions and the characteristics of light hydrocarbons show that the natural gases in the studied area are dominated by coal-derived gas and contain a small amount of oil-associated and mixed-type gas. According to the gas source comparison results, it is basically confirmed that the coal-derived gas is from the mature to highly mature source rocks of the Lower Urho formation, and the oil-associated gas is from the mature to highly mature source rocks of the Fengcheng formation.

Gas once migrated vertically in the gas-bearing formations, leading to the mixing of oil-associated and coal-derived gases, as well as the mixing of alkane gases of the same genetic type formed at different stages and possibly causing a reversed carbon isotopic series. While the components and carbon isotopic composition of the natural gases in the Jurassic Sangonghe formation vary with the maturity of the source rocks, these features of the Carboniferous gases are mainly affected by the gas diffusion migration after reservoir formation. Natural gas migration characteristics indicate the shallow layer (e.g., the Cretaceous) in the eastern belt around the Penyijingxi sag may be a favorable area for future oil and gas exploration, which is suitable for searching for secondary hydrocarbon reservoirs.

Author Contributions: Methodology, J.Q. and X.D.; Validation, M.Z. (Minghui Zhou) and T.G.; Investigation, K.L.; Resources, H.L.; Writing–original draft, K.L.; Writing–review & editing, K.L.; Supervision, M.Z. (Ming Zhao) and X.D.; Project administration, M.Z. (Ming Zhao); Funding acquisition, H.L. All authors have read and agreed to the published version of the manuscript.

Funding: This work was supported by major projects of PetroChina Science and Technology (2021DJ0206).

Data Availability Statement: Restrictions apply to the availability of these data. With the permission of Xinjiang Oilfield, it can be obtained from the authors.

Conflicts of Interest: The authors declare no conflict of interest.

Appendix A

Table A1. Natural gas compositions in the eastern belt around the Penyijingxi Sag, Junggar Basin.

Location	Well	Formation	Depth/m	Chemical Composition/%							Carbon Isotopic Composition/‰ (PDB)			
				N_2	CO_2	CH_4	C_2H_6	C_3H_8	C_4H_{10}	C_5H_{12}	$\delta^{13}C_1$	$\delta^{13}C_2$	$\delta^{13}C_3$	$\delta^{13}C_4$
MBB	M121	J1s	4222.00	1.68	0.02	93.34	3.10	0.93	0.57	0.21	nd	nd	nd	nd
MBB	M121	J1s	4254.50	1.60	0.15	91.58	4.02	1.37	0.81	0.28	nd	nd	nd	nd
MBB	M109	J1s	4158.00	0.69	0.67	93.30	3.42	0.98	0.59	0.21	nd	nd	nd	nd
MBB	M113	J1s	4205.00	1.07	0.14	92.70	3.51	1.19	0.84	0.35	nd	nd	nd	nd
MBB	M115	J1s	4204.00	1.43	0.20	88.16	5.39	2.23	1.70	0.63	nd	nd	nd	nd
MBB	M116	J1s	4195.00	2.68	0.23	91.11	3.40	1.19	0.80	0.32	nd	nd	nd	nd
MBB	M117	J1s	4237.50	1.89	0.30	90.63	3.98	1.48	1.04	0.42	nd	nd	nd	nd
MBB	M119	J1s	4258.25	2.04	0.18	90.88	3.98	1.41	0.87	0.31	nd	nd	nd	nd
MBB	M119	J1s	4236.00	1.69	0.19	92.17	3.55	1.23	0.75	0.25	nd	nd	nd	nd
MBB	M003	J1s	3915.00	1.08	0.59	92.40	3.61	1.20	0.74	0.24	−41.07	−29.26	−27.76	−26.95
MBB	M003	J1s	3975.00	2.86	0.29	88.77	4.29	1.65	nd	nd	−35.25	−27.46	−25.92	−25.87
MBB	MB2	J1s	3921.00	2.68	0.41	92.98	2.52	0.77	nd	nd	−42.89	−30.04	−27.26	−27.02
MBB	MB2	J1s	3921.00	2.72	0.51	91.22	3.29	1.09	nd	nd	−44.12	−29.38	−26.33	−26.58
MBB	MB5	J1s	3726.20	2.71	0.00	88.16	5.19	1.73	nd	nd	−34.80	−26.93	−26.14	−26.28
MBB	MB10	J1s	3666.00	3.27	0.41	88.24	4.26	1.69	nd	nd	−41.72	−27.90	−26.59	−26.62
MBS	M16	J1s	4047.25	1.60	0.40	89.90	4.30	1.47	1.05	0.53	−37.56	−27.52	−26.73	−26.76
MBS	QS1	J1s	3944.50	1.35	0.70	89.90	4.34	1.53	1.10	0.52	−37.40	−27.55	−26.72	−25.94
MBS	QS1	J1s	3944.75	1.65	0.46	90.66	4.33	1.48	0.92	0.27	−35.60	−26.14	−25.53	−25.14
MBS	QS2	J1s	3981.00	1.09	0.45	91.18	4.31	1.47	0.94	0.33	−37.49	−27.54	−26.71	−26.80
MBS	QS4	J1s	4014.25	1.56	0.31	90.79	4.39	1.48	0.91	0.33	−37.82	−27.57	−26.72	−26.97
MSWB	M101	J1s	4204.00	2.95	0.62	89.51	4.25	1.47	0.84	0.24	−36.64	−27.21	−26.72	−26.75
SXB	S006	J1s	3577.00	0.92	0.68	91.12	4.38	1.47	0.90	0.33	nd	nd	nd	nd
SXB	S006	C	4373.00	4.35	0.21	88.82	3.70	1.07	1.08	0.54	−41.62	−28.68	−25.88	−25.40
SXB	S007	C	4408.50	11.95	0.09	71.36	5.32	4.36	4.55	1.78	−40.58	−30.17	−26.85	−26.75
SXB	SX1	C	4438.00	5.21	0	78.97	6.52	3.96	3.95	1.39	−33.43	−26.69	−26.00	−25.44
SXB	SX1	C	4473.00	5.49	0.37	77.25	7.92	3.73	3.70	1.55	−35.36	−27.50	−26.63	−26.37
SXB	S015	J1s	nd	4.68	1.07	75.10	9.11	4.04	4.04	1.49	−42.5	−29.31	−26.87	−26.47
SXB	SX8	J1s	nd	1.25	0.63	84.04	7.61	2.98	1.97	0.77	−34.44	−26.06	−24.66	−25.61
SXB	SX14	J1s	nd	3.63	0.82	75.41	8.45	4.72	3.45	1.40	−36.98	−27.75	−27.20	−27.96
MBB	MB11	J1s	3710.75	1.31	0.82	84.98	6.69	3.01	1.93	0.75	−37.11	−28.19	−26.78	−26.7
MBB	MB2	J1s	3907.00	2.81	0.07	91.56	3.40	1.13	0.64	0.23	−35.65	−26.84	−26.16	−26.44
MBB	M003	J1s	3971.50	3.39	0.60	89.31	4.58	1.31	0.64	0.18	−37.82	−26.58	−24.68	−23.64

Table A1. *Cont.*

Location	Well	Formation	Depth/m	Chemical Composition/%							Carbon Isotopic Composition/‰ (PDB)			
				N_2	CO_2	CH_4	C_2H_6	C_3H_8	C_4H_{10}	C_5H_{12}	$\delta^{13}C_1$	$\delta^{13}C_2$	$\delta^{13}C_3$	$\delta^{13}C_4$
MBB	MB9	J1s	3761.25	1.82	0.35	90.57	4.42	1.37	0.97	0.50	−42.92	−27.11	−25.73	−26.00
MBB	MB9	J1s	3778.00	1.71	1.29	84.56	5.75	2.67	1.90	0.93	−45.57	−31.39	−28.67	−27.47
MBB	M005	J1s	3890.25	2.36	0.42	86.76	6.41	2.38	1.59	0.08	−44.08	−30.16	−27.67	−27.4
MBB	M006	J1s	3759.25	2.01	0.45	85.84	6.38	2.71	1.95	0.66	−39.46	−28.18	−28.01	−27.3
MBB	MB5	J1s	3726.20	3.96	0.22	89.21	4.46	1.12	0.81	0.23	−35.58	−27.41	−26.19	−26.5
MBB	M108	J1s	4179.00	2.74	0.30	89.66	3.53	1.10	0.75	0.37	−35.28	−25.74	−25.28	−25.8
MBB	M109	J1s	4185.00	1.81	0.22	91.97	4.16	1.10	0.50	0.12	−38.96	−24.66	−23.56	nd
MBB	M11	J1s	4139.00	3.60	1.49	88.58	3.30	1.01	0.68	0.32	−35.15	−25.71	−25.13	−25.64
MBB	M11	J1s	4177.00	1.65	0.27	91.82	3.86	1.33	0.77	0.22	−34.84	−27.09	−26.35	−26.61
MBB	M7	J1s	4227.50	2.40	0.47	90.92	3.54	1.19	0.80	0.36	−35.72	−26.43	−25.85	−26.37
MBB	M7	J1s	4260.00	3.65	0.50	89.99	3.33	1.15	0.71	0.31	−37.88	−27.90	−27.17	−27.66
MBB	M8	J1s	4233.00	1.47	0.51	91.43	3.56	1.07	0.70	0.36	−35.82	−26.21	−25.39	−25.46
MBB	M8	J1s	4265.50	1.09	0.42	87.70	5.86	2.23	1.53	0.62	−34.69	−25.91	−25.33	−25.74
MBS	M16	J1s	4041.00	2.69	0.62	87.44	5.62	1.77	0.90	0.32	−36.54	−26.48	−25.03	−26.26
MBS	M171	J1s	4472.85	1.45	0.40	90.45	4.52	1.58	0.98	0.37	−36.59	−26.58	−25.57	−26.19
MBS	M17	J1s	4161.50	1.86	0.57	91.20	4.02	1.07	0.60	0.24	−36.9	−26.86	−25.64	−26.38
MBS	M12	J1s	4235.00	3.25	0.66	80.44	6.96	4.14	2.72	0.95	−34.14	−27.30	−26.29	−26.59
MBS	M17	J1s	4192.00	1.55	0.66	73.88	10.90	5.96	4.38	1.57	−35.93	−26.49	−24.36	−25.42
MSWB	M101	J1s	4209.00	3.01	0.41	88.76	4.35	1.56	1.07	0.48	−36.81	−27.31	−26.32	−26.79
MSWB	M102	J1s	4251.00	2.71	0.52	88.13	4.70	1.92	1.21	0.48	−36.11	−27.51	−26.40	−26.52
MSWB	M103	J1s	4250.50	2.59	0.58	87.65	4.69	1.98	1.43	0.62	−36.66	−27.28	−26.647	−26.98
MSWB	P5	J1s	4250.00	3.25	0.57	87.49	4.49	1.86	1.20	0.45	−41.43	−28.04	−27.03	−27.42

Note: nd means no data, C means Carboniferous, J1s means Jurassic Sangonghe Formation, MBB means Mobei bulge, MSWB maens Mosuowan bulge, SXB means Shixi bulge, MBS means Mobei slope.

References

1. Glasby, G.P. Abiogenic origin of hydrocarbons: An historical overview. *Resour. Geol.* **2006**, *56*, 83–96. [CrossRef]
2. Dai, J.; Gong, D.; Ni, Y.; Huang, S.; Wu, W. Stable carbon isotopes of coal-derived gases sourced from the Mesozoic coal measures in China. *Org. Geochem.* **2014**, *74*, 123–142. [CrossRef]
3. Song, Y.; Xu, Y.C. Origin and identification of natural gases. *Pet. Explor. Dev.* **2005**, *32*, 24–29.
4. Milkov, A.V. Methanogenic biodegradation of petroleum in the West Siberian Basin (Russia): Significance for formation of giant Cenomanian gas pools. *AAPG Bull.* **2010**, *94*, 1485–1541. [CrossRef]
5. Hutcheon, I.; Krouse, H.R.; Abercrombie, H.J. Controls on the origin and distribution of elemental sulfur, H_2S, and CO_2 in Paleozoic hydrocarbon reservoirs in Western Canada. *ACS Symp. Ser.* **1995**, *612*, 426–438.
6. Arrouvel, C.; Prinzhofer, A. Genesis of natural hydrogen: New insights from thermodynamic simulations. *Int. J. Hydrogen Energy* **2021**, *46*, 18780–18794. [CrossRef]
7. Milkov, A.V.; Giuseppe, E. Revised genetic diagrams for natural gases based on a global dataset of >20,000 samples. *Org. Geochem.* **2018**, *125*, 109–120. [CrossRef]
8. Dai, J.X.; Huang, S.P. Discussion on the carbon isotopic reversal of alkane gases from the Huanglong Formation in the Sichuan Basin, China. *Acta Pet. Sin.* **2010**, *31*, 710–717.
9. Des Marais, D.J.; Donchin, J.H.; Nehring, N.L.; Truesdell, A.H. Molecular carbon isotopic evidence for the origin of geothermal hydrocarbons. *Nature* **1981**, *292*, 826–828. [CrossRef]
10. Tilley, B.; Muehlenbachs, K. Isotope reversals and universal stages and trends of gas maturation in sealed, self-contained petroleum systems. *Chem. Geol.* **2013**, *339*, 194–204. [CrossRef]
11. Dai, J.; Xia, X.; Qin, S.; Zhao, J. Origins of partally reversed alkane $\delta^{13}C$ values for biogenic gases in China. *Org. Geochem.* **2004**, *35*, 405–411. [CrossRef]
12. Hosgormez, H.; Etiope, G.; Yalin, M.N. New evidence for a mixed inorganic and organic origin of the Olympic Chimaera fire (Turkey): A large onshore seepage of abiogenic gas. *Geofluids* **2008**, *8*, 263–273. [CrossRef]
13. Ogbesejana, A.B.; Bello, O.M.; Ali, T. Origin and depositional environments of source rocks and crude oils from Niger Delta Basin: Carbon isotopic evidence. *China Geol.* **2020**, *3*, 602–610. [CrossRef]
14. Schoell, M. The hydrogen and carbon isotopic composition of methane from natural gases of various origins. *Geochim. Cosmochim. Acta* **1980**, *44*, 649–661. [CrossRef]
15. Kotarba, M. Isotopic geochemistry and habitat of the natural gases from the Upper Carboniferous Žacleř coal-bearing formation in the Nowa Ruda coal district (Lower Silesia, Poland). *Org. Geochem.* **1990**, *16*, 549–560. [CrossRef]
16. Battani, A.; Sarda, P.; Prinzhofer, A. Basin scale natural gas source, migration and trapping traced by noblegases and major elements: The Pakistan Indus basin. *Earth Planet. Sci. Lett.* **2000**, *181*, 229–249. [CrossRef]
17. Prinzhofer, A.; Mello, M.R.; Freitas, L.; Takaki, T. New geochemical characterization of natural gas and its use in oil and gas evaluation. *AAPG Mem.* **2000**, *73*, 107–119.
18. Allan, U.S. Model for hydrocarbon migration and entrapment within faulted structures. *AAPG Bull.* **1989**, *73*, 803–811.
19. Hillman, J.I.; Cook, A.E.; Daigle, H.; Nole, M.; Malinverno, A.; Meazell, K.; Flemings, P.B. Gas hydrate reservoirs and gas migration mechanisms in the Terrebonne Basin, Gulf of Mexico. *Mar. Pet. Geol.* **2017**, *86*, 1357–1373. [CrossRef]
20. Wanner, P.; Hunkeler, D. Isotope fractionation due to aqueous phase diffusion–What do diffusion models and experiments tell?–A review. *Chemosphere* **2019**, *219*, 1032–1043. [CrossRef]
21. Losh, S.; Walter, L.; Meulbroek, P.; Martini, A.; Whelan, J. Reservoir Fluids and Their Migration into the South Eugene Island Block 330 Reservoirs, Offshore Louisiana. *AAPG Bull.* **2002**, *86*, 1463–1488.
22. Prinzhofer, A.; Battani, A. Gas isotopes tracing: An important tool for hydrocarbons exploration. *Oil Gas Sci. Technol.* **2003**, *58*, 299–311. [CrossRef]
23. Schloemer, S.; Krooss, B.M. Molecular transport of methane, ethane and nitrogen and the influence of diffusion on the chemical and isotopic composition of natural gas accumulations. *Geofluids* **2010**, *4*, 81–108. [CrossRef]
24. Prinzhofer, A.; Neto, E.; Battani, A. Coupled use of carbon isotopes and noble gas isotopes in the Potiguar basin (Brazil): Fluids migration and mantle influence. *Mar. Pet. Geol.* **2010**, *27*, 1273–1284. [CrossRef]
25. Prinzhofer, A.; Mello, M.R.; Takaki, T. Geochemical Characterization of Natural Gas: A Physical Multivariable Approach and Its Applications in Maturity and Migration Estimates. *AAPG Bull.* **2000**, *84*, 1152–1172.
26. Bourg, I.C.; Sposito, G. Isotopic fractionation of noble gases by diffusion in liquid water: Molecular dynamics simulations and hydrologic applications. *Geochim. Cosmochim. Acta* **2008**, *72*, 2237–2247. [CrossRef]
27. Sun, P.; Wang, Y.; Leng, K.; Li, H.; Ma, W.; Cao, J. Geochemistry and origin of natural gas in the eastern Junggar Basin, NW China. *Mar. Pet. Geol.* **2016**, *75*, 240–251. [CrossRef]
28. Yang, H.B.; He, W.J.; Jia, X.Y. *The Fourth Evaluation of Oil and Gas Resources in Junggar Basin*; Internal Report of Exploration and Development Research Institute of Xinjiang Oilfield Company: Karamay, China, 2016.
29. IEA. *Offshore Energy Outlook*; IEA: Paris, France, 2018.
30. Tao, K.; Cao, J.; Wang, Y.; Ma, W.; Xiang, B.; Ren, J.; Zhou, N. Geochemistry and origin of natural gas in the petroliferous Mahu sag, northwestern Junggar Basin, NW China: Carboniferous marine and Permian lacustrine gas systems. *Org. Geochem.* **2016**, *100*, 62–79. [CrossRef]

31. Huayao, Z.; Fang, H.; Bin, Z.B.C. History of hydrocarbon-filling and remigrating in hinterland of the Junggar Basin. *Chin. J. Geol.* **2005**, *40*, 499–509.
32. Ma, W.; Wei, Y.; Li, X.; Tao, S.; Li, Y.; Zhao, Z. Accumulation process and control factors of Jurassic-Cretaceous distant-source and secondary-filled reservoirs in the hinterland of Junggur Basin. *Acta Sci. Nat. Univ. Pekin.* **2018**, *54*, 1195–1204.
33. Zhu, G.; Su, J.; Yang, H.; Wang, Y.; Fei, A.; Liu, K.; Zhu, Y.; Hu, J.; Zhang, B. Formation mechanisms of secondary hydrocarbon pools in the Triassic reservoirs in the northern Tarim Basin. *Mar. Pet. Geol.* **2013**, *46*, 51–66. [CrossRef]
34. Lei, J.; Worden, R.H.; Cai, C.F. Thermochemical sulfate reduction and fluid evolution of the Lower Triassic Feixianguan Formation sour gas reservoirs, northeast Sichuan Basin, China. *AAPG Bull.* **2014**, *98*, 947–973.
35. Volk, H.; George, S.C.; Kempton, R.H.; Liu, K.; Ahmed, M.; Ambrose, G.J. Petroleum migration in the Georgina Basin: Evidence from the geochemistry of oil inclusions and bitumens. In Proceedings of the Central Australian Basins Symposium (CABS). Northern Territory Geological Survey, Alice Springs, Northern Territory, Australia, 16–18 August 2007; pp. 282–303.
36. Ali, A.; Younas, M.; Ullah, M.; Hussain, M.; Toqeer, M.; Bhatti, A.S.; Khan, A. Characterization of secondary reservoir potential via seismic inversion and attribute analysis: A case study. *J. Pet. Sci. Eng.* **2019**, *178*, 272–293. [CrossRef]
37. Jahn, B.M.; Wu, F.; Chen, B. Massive granitoid generation in Central Asia: Nd isotope evidence and implication for continental growth in the Phanerozoic. *Episodes* **2000**, *23*, 82–92. [CrossRef] [PubMed]
38. Windley, B.F.; Alexeiev, D.; Xiao, W.; Kröner, A.; Badarch, G. Tectonic models for accretion of the Central Asian Orogenic Belt. *J. Geol. Soc.* **2007**, *164*, 31–47. [CrossRef]
39. Liu, H.L.; Yin, H.; Imin, A.; Ding, X. Origin and preservation of deep natural gas in the lower assemblage of the western Junggar Basin. *J. China Univ. Min. Technol.* **2022**, *51*, 148–159.
40. Chen, J.P.; Wang, X.L.; Deng, C.P.; Liang, D.G.; Zhang, Y.Q.; Zhao, Z.; Wang, Y.T. Geochemical features of source rocks and crude oil in the Junggar Basin, northwestem China. *Acta Geol. Sin.* **2016**, *90*, 37–67.
41. Saadati, H.; Al-Iessa, H.J.; Alizadeh, B.; Tarhandeh, E.; Jazayeri, M.H.; Bahrami, H.; Rashidi, M. Geochemical characteristics and isotopic reversal of natural gases in eastern Kopeh-Dagh, NE Iran. *Mar. Pet. Geol.* **2016**, *78*, 76–87. [CrossRef]
42. Qiu, N.S.; Yang, H.B.; Wang, X.L. Tectonic-thermal evolution in the Junggar Basin. *Chin. J. Geol.* **2002**, *37*, 423–429.
43. Milkov, A.V. Worldwide distribution and significance of secondary microbial methane formed during petroleum biodegradation in conventional reservoirs. *Org. Geochem.* **2011**, *42*, 184–207. [CrossRef]
44. Mango, F.D. The light hydrocarbons in petroleum: A critical review. *Org. Geochem.* **1997**, *26*, 417–440. [CrossRef]
45. Hu, T.L.; Ge, B.X.; Zhang, Y.G.; Liu, B. Development and application of fingerprint parameters of source rock adsorbed hydrocarbon and natural gas light hydrocarbon. *Pet. Geol. Exp.* **1990**, *12*, 375–394,450.
46. Leythaeuser, D.; Schaefer, R.; Cornford, C.; Weiner, B. Generation and migration of light hydrocarbons (C_2–C_7) in sedimentary basins. *Org. Geochem.* **1979**, *1*, 191–204. [CrossRef]
47. Qian, H.T.; Su, D.X.; Ablimit, I.; Wang, X.Y.; Li, Z.H.; Wang, G.D. Petroleum geological characteristics and exploration potential in slope area of Well Pen-1 Western Depression in Junggar Basin. *Nat. Gas Geosci.* **2021**, *32*, 551–561.
48. Chen, J.P.; Sun, Y.G.; Zhong, N.N.; Huang, Z.K.; Deng, C.P. Lacustrine facies hydrocarbon expulsion efficiency of hydrocarbon source rock and hydrocarbon expulsion model. In Proceedings of the Fourteenth China Mineral Rock Geochemistry Academic Annual Conference, Nanjing, China, 21 April 2013.
49. Harry, D.J. Three common source rock evaluation errors made by geologists during prospect or play appraisals. *AAPG Bull.* **2009**, *93*, 341–356.
50. Mango, F.D. The origin of light hydrocarbons in petroleum: A kinetic test of the steady-state catalytic hypothesis. *Geochim. Cosmochim. Acta* **1990**, *54*, 1315–1323. [CrossRef]
51. Wu, M. *Geochemical Study on Hydrocarbon Accumulation in Deep Strata of the Central Junggar Basin, Northwest China*; Nanjing University: Nanjing, China, 2012.
52. Schoell, M. Genetic characterization of natural gases. *AAPG Bull.* **1983**, *67*, 2225–2238.
53. Chen, J.; Wang, X.; Chen, J.; Ni, Y.; Xiang, B.; Liao, F.; He, W.; Yao, L.; Li, E. New equation to decipher the relationship between carbon isotopic composition of methane and maturity of gas source rocks. *Sci. China Earth Sci.* **2021**, *64*, 470–493. [CrossRef]
54. Prinzhofer, A.; Pernaton, R. Isotopically light methane in natural gas: Bacterial imprint or diffusive fractionation? *Chem. Geol.* **1997**, *142*, 193–200. [CrossRef]
55. Hou, L.; Wang, J.; Kuang, L.; Zhang, G.; Liu, L.; Kuang, J. Provenance Sediments and Its Exploration Significance-A Case from Member 1 of Qingshuihe Formation of Lower Cretaceous in Junggar Basin. *Earth Sci. Front.* **2009**, *16*, 337–348. [CrossRef]
56. Kou, C.H. *Origins and Accumulation Model of Hydrocarbon in Deep Strata of the Central Junggar Basin, Northwestern China*; Nanjing University: Nanjing, China, 2017.
57. Cheshmeh Sefidi, A.; Ajorkaran, F. A novel MLP-ANN approach to predict solution gas-oil ratio. *Pet. Sci. Technol.* **2019**, *37*, 2302–2308. [CrossRef]